Suspension Polymerization of Poly(methyl methacrylate)/Clay Nanocomposites

Nigel Clarke,[1] Lian R. Hutchings,[1] Ian Robinson,[2] Judith A. Elder,[1] Stephen A. Collins[1]

[1]*Department of Chemistry, University of Durham, Durham DH1 3LE, United Kingdom*
[2]*Lucite International UK, Limited, Wilton Centre, Wilton TS10 4RF, United Kingdom*

Received 7 October 2008; accepted 25 January 2009
DOI 10.1002/app.30128
Published online 2 April 2009 in Wiley InterScience (www.interscience.wiley.com).

ABSTRACT: Polymer/clay nanocomposites (PCNs) of poly(methyl methacrylate) and an organically modified clay, Cloisite 15a, were synthesized *in situ* with a suspension polymerization technique. The amount of clay present in the PCNs was varied to provide a better understanding of the effect of the clay on the properties of the polymer matrix. However, unexpectedly, we found that the concentration of clay had a dramatic impact on the molecular weight of the polymer matrix, and a relationship between the clay concentration and polymer molecular weight was determined. The PCNs were characterized with size exclusion chromatography (SEC), X-ray diffraction, transmission electron microscopy, and oscillatory shear rheology. From oscillatory shear rheology, the full master curves for the PCNs were obtained by application of the time–temperature superposition principle. To enable the effect of the clay on the rheology to be quantified, the experimental data was compared to the time-dependent diffusion model of des Cloizeaux for polydisperse polymer melts, which enabled the polydispersity to be incorporated through the use of the molecular weight distribution obtained via SEC. © 2009 Wiley Periodicals, Inc. J Appl Polym Sci 113: 1307–1315, 2009

Key words: clay; molecular weight distribution/molar; nanocomposites; rheology

INTRODUCTION

Polymer/clay nanocomposites (PCNs) have become an area of sustained interest with several recent reviews on PCNs in the literature.[1–3] Furthermore, it has been reported that increases in the thermal stability,[4–7] flame retardency,[8–11] tensile strength,[12–14] and glass-transition temperature[15–18] have been achieved in PCNs compared to the values for pure polymer matrices. One of the advantages of clay is that smaller percentages of clay (<10%), compared to conventional fillers, are required to provide improved material properties. For example, Fornes et al.[19] compared the Young's modulus of glass fiber and clay nanocomposites and found that clay provided better reinforcement than the glass fiber, with only 7.2 wt % clay needed to double the Young's modulus, whereas 20 wt % glass fiber was required to obtain a similar effect.

Montmorillonite, which is one of the most common clays used in polymer nanocomposites, has two different active sites that enable it to act as a Brønsted and Lewis acid catalysist.[20] It is well known that the surfaces of montmorillonites are negatively charged because of impurities that are present in the crystalline structure. These active sites are usually charge-balanced by the addition of a cation, for example, H_3O^+ or Na^+. When the negative charge is neutralized by a proton (H^+), the clay surface acts as a Brønsted acid site; as the proton is only loosely bound, it can be easily donated. Lewis acid sites can also be found on the rim of the clay platelets. The positive rim charge arises from the octahedral Al^{3+} cations located at the rim of the platelet. The positive charge is usually neutralized by hydroxide ions.

Previous studies[21–24] of PCNs created *in situ,* that is, where the monomer is polymerized in the presence of the clay, have shown changes in the molecular weight for polymerizations carried out in the presence of clay as compared to polymerizations carried out in the absence of clay. Kim et al.[21] reported the molecular weights for the polymer matrix of nanocomposites prepared via suspension polymerization in the presence of 2–8% organically modified montmorillonite. The data showed an increase in molecular weight compared to the pure poly(methyl methacrylate) (PMMA), with the molecular weight ranging from 333,000 to 638,000 g/mol. The molecular weight appeared to have no clear dependence on the clay concentration, and Kim et al.[21] concluded that montmorillonite did not affect the kinetics of the polymerization process. A change in the

Correspondence to: J. A. Elder (judith.elder@durham.ac.uk).

molecular mass was also observed by Lee and Jang,[22] who used an organically modified bentonite clay. The clay was again shown to cause an increase in the molecular mass; however, this time, a large mass (20–50 wt %) of clay was used.

A bimodal distribution in the molecular weight of the matrix polymer has also been reported,[23,24] and this was attributed to the heterogeneous reaction conditions caused by the clay. It was suggested that the propagating PMMA chains in close proximity to the clay had a high probability of reacting with the clay, and this resulted in a lower molecular weight fraction, whereas the propagating PMMA chains in the bulk (away from the clay) were less likely to be terminated by the clay, which generated the higher molecular weight part of the distribution. As a result of this phenomenon, it is to be expected that the concentration of clay will affect the molecular weight of the matrix when free-radical polymerization techniques are used.

If the presence of clay during polymerization results in a change in the molecular weight distribution of the resulting polymer matrix, it is important to distinguish between the effect of molecular weight and the effect of the presence of clay on the resulting physical properties of the PCNs; the latter can easily be masked by the former.[19,25] The rheology of a PCN is an important physical property, particularly with regard to processing, which can be affected by either the addition of clay and/or the molecular weight distribution of the matrix polymer. In this article, we show that one way to distinguish between the two effects is to predict the rheology of the matrix molecular weight with theoretical models.

The theory of reptation was first reported by de Gennes,[26] who proposed that the entanglements surrounding a polymer chain can be modeled as a tube in which the chain can diffuse along, reptate, and the reptation time was defined as the time taken for the chain to diffuse out of a tube of a certain length, where the length was dependent on the chain length. Doi and Edwards[27] used the idea of reptation to develop a model to predict the rheological behavior of linear monodisperse polymers. It has since been found that other more complex chain relaxation processes, such as tube length fluctuation and constraint release mechanisms, are also necessary to provide qualitative agreement between theory and experiment.[28]

To model the rheology of polymers produced by free-radical polymerization, the polydispersity index (PDI) of the material needs to be considered. Van Ruymbeke et al.[29] predicted the rheology for monodisperse, bidisperse, and polydisperse polystyrene samples with the use of experimentally determined molecular weight distributions obtained by size exclusion chromatography (SEC). Van Ruymbeke et al.[29] found that a model by des Cloizeaux[30] provided the best fit to the experimental data. This model is based on a time-dependent process, with a relaxation function [$F_{TDD}(t,M)$] given by

$$F_{TDD}(t,M) = \frac{8}{\pi^2}\sum_{n=0}^{\infty}\frac{1}{(2n+1)}\exp\left\{-(2n+1)^2\left[\frac{t}{\tau_{rep}(M)} + \frac{\tau_i(M)}{\tau_{rep}(M)}\left(\sum_{n=1}^{\infty}\left(\frac{1-\exp\left(-n^2\frac{t}{\tau_i(M)}\right)}{n^2}\right)\right)\right]\right\} \quad (1)$$

where M is the molecular weight, t is the time, τ_{rep} is the reptation relaxation time, and τ_i is an intermediate relaxation time that lies between τ_{rep} and the Rouse relaxation time (τ_R).[30] To include the effects of PDI, the relaxation function would need to be calculated for a number of different values of M, and the relaxation modulus can be then obtained with the double-reptation concept as a mixing rule. Double reptation was derived independently by des Cloizeaux[31] and Tsenoglou,[32] as shown in eq. (2), where G_{rep} is the reputation relaxation modulus; $w(M)$ is equal to $W(M)/(d \log M)$ and $dW(M)$ is the weight fraction of chains with a molecular weight below; M, G_N^0 is the plateau modulus, and β is a constant typically assumed to have a value of 2.0,[31–33] although some studies have shown that, for highly entangled melts, the value of β may in fact be larger:[29,34]

$$G_{rep}(t) = G_N^0\left(\int_{\log M_e}^{\infty}(F(t,M)w(M)d\log M)\right)^{\beta} \quad (2)$$

The Rouse region is modeled with the Rouse relaxation modulus (Grouse) for an entangled polymer melt, as shown in eq. (3), where N is the number of entanglements in a polymer chain. This is in a similar fashion to van Ruymbeke et al.[29] The final issue to consider is the calculation of the storage modulus (G') and loss modulus (G'') from the relaxation function. One usually calculates G' and G'' by carrying out a Fourier transform, but, in this case, Fourier transform would be computationally intensive and unnecessary; therefore, the Schwarzl relation[35] is used:

$$G_{Rouse}(t) = G_N^0\sum_{p=N}^{\infty}\frac{1}{N}\exp\left(\frac{-p^2t}{\tau_R(M)}\right) + \frac{1}{3}G_N^0\sum_{p=1}^{N}\frac{1}{N}\exp\left(\frac{-p^2t}{\tau_R(M)}\right) \quad (3)$$

The aim of this study was to investigate the dual effects that the presence of clay has on the molecular weight distribution and the physical properties of the resulting PCN when PMMA is polymerized by a suspension free-radical polymerization mechanism in the presence of clay nanoparticles through the

variation of the amount of clay added. A series of PCNs were prepared and characterized by SEC, transmission electron microscopy (TEM), and rheology. Specifically, the relationship between the physical properties and the concentration of clay were assessed to see if the changes were due to the presence of the clay platelets alone or whether changes in the molecular weight distribution contributed to any of the changes in the physical properties.

EXPERIMENTAL

Materials

Cloisite 15a (C15a) was a montmorillonite clay that was organically modified with dimethyl dehydrogenated tallow quaternary ammonium salt and was purchased from Southern Clay (Cheshire, United Kingdom). Methyl methacrylate (MMA), the suspending agent [a 1% aqueous solution of poly(2-methyl-2-propenoic acid) sodium salt] and the initiator, 2,2-azobis(2-methylpropionitrile) (AIBN), were kindly supplied by Lucite International (Wilton, United Kingdom) and were used as received. A comonomer of ethyl propenoate was used in the suspension polymerization and was purchased from Sigma Aldrich (Gillingham, United Kingdom). To control the molecular weight, a chain-transfer agent (CTA) of 1-dodecanethiol purchased from Fluka (United Kingdom) was used.

Suspension polymerization of PMMA

The MMA monomer (4 mol, 400 g) was dispersed in 2 L of deionized water in a three-necked, round-bottom flask. CTA (9.9 mmol, 2 g) was added, along with 0.12 mol (12 g) of ethyl propenoate, 100 g of suspending agent, and 6.1 mmol (1 g) of AIBN. The pH of the aqueous phase was maintained at pH 10 through the use of a buffer solution.[36] The suspension was then vigorously stirred with an overhead mechanical stirrer and was heated to reflux (83°C) under a blanket of nitrogen. Once the reflux had receded (ca. 30 min), the reaction was stirred at 90°C for 2 h to consume any residual monomer and then cooled to ambient temperature. The PMMA beads were filtered off, washed with deionized water, and then dried in a vacuum oven at 80°C for 24 h.

Suspension polymerization of the PMMA nanocomposites

C15a (4 wt %, 16 g) was added to 4.0 mol (400 g) of MMA monomer in a three-necked, round-bottom flask; this solution was stirred vigorously with an overhead mechanical stirrer for 15 min, after which 2 L of deionized water was added. CTA (9.9 mmol, 2 g) was added, along with 0.12 mol (12 g) of ethyl propenoate, 100 g of suspending agent, and 6.1 mmol (1 g) of AIBN. The pH of the aqueous phase was maintained at pH 10 through the use of a buffer solution.[36] The suspension was vigorously stirred with an overhead mechanical stirrer and was heated to reflux (83°C) under a blanket of nitrogen. Once the reflux had receded (ca. 30 min), the reaction was heat-treated at 90°C for 2 h to remove any residual monomer and then cooled to ambient temperature. The PMMA beads where filtered off, washed with deionized water, and then dried in a vacuum oven at 80°C for 24 h.

The PMMA nanocomposites containing 0.05, 0.1, 0.25, 0.5, 1, and 2 wt % C15a were also synthesized as discussed previously. To help understand the change in molecular weight discussed later, 0.25% C15a samples where also prepared with 0 and 19.8 mmol (4 g) of CTA.

Characterization

The molecular weight distribution was determined with triple-detection SEC. A Viscotek (Berkshire, United Kingdom) TDA 302 with refractive index, viscosity, and light-scattering detectors and two 300-mm PLgel 5-μm mixed C columns was used. The eluent was tetrahydrofuran, which was used at a flow rate of 1.0 mL/min at a temperature of 35°C. The detectors were calibrated with a single narrow molecular weight distribution polystyrene standard. The sample (4.5 mg) was dissolved in tetrahydrofuran and then filtered through a 0.2-μm syringe filter to remove any large clay aggregates, which could potentially block the SEC columns. For consistency, the pure PMMA samples were also filtered.

The morphology of the PCNs were characterized with X-ray diffraction (XRD) and TEM. XRD was carried out on the PCN samples, which were pressed in a heat press at 200°C for 15 min. A Siemens (United Kingdom) D5000 diffractometer, equipped with a Cu Kα source generating X-rays with a wavelength of 1.54 Å, was used. Microscopy was carried out with a Philips (Cambridge, United Kingdom) CM12 TEM with an accelerating voltage of 120 kV, and images were captured with a Gatan (Abingdon, United Kingdom) 2500 camera. Samples 65 nm thick were cut at room temperature with a Reichert (United Kingdom) Ultracut-E ultra microtome and placed onto copper grids. Because there was a sufficient difference in the electron density between the PMMA and the clay, no staining was required.

Oscillatory rheological experiments were carried out on the PCNs and PMMA, which was used as a reference. A TA Instruments (West Sussex, United Kingdom) AR2000 rheometer fitted with 25-mm parallel plates in an environmental test chamber, to ensure a constant temperature, was used. We prepared the samples by heat-pressing the beads into

TABLE I
Molecular Weight Data Obtained from the GPC of the PMMA and PMMA/C15a Nanocomposites

	Clay (wt %)	CTA (mmol)	M_w (g/mol)	M_n (g/mol)	PDI
PMMA	0		97,000	54,000	1.8
0.05% C15a	0.05	9.9	137,000	60,000	2.3
0.1% C15a	0.1	9.9	313,000	127,000	2.5
0.25% C15a	0.25	9.9	660,000	234,000	2.8
0.5% C15a	0.5	9.9	802,000	206,000	3.9
1% C15a	1	9.9	800,000	209,000	3.8
2% C15a	2	9.9	803,000	220,000	3.7
4% C15a	4	9.9	806,000	257,000	3.1

M_n = number-average molecular weight.

25-mm diameter disks with a thickness of 1 mm. Heat pressing was carried out at 200°C for 15 min. Oscillatory measurements were obtained with stress control with a frequency range of 0.1–100 rad/s. Measurements were carried out at temperatures of 140–245°C at 15°C intervals. The data was subsequently shifted with the time–temperature superposition principle[37] to obtain the full master curve.

RESULTS AND DISCUSSION

Molecular weight

The molecular weight data of the PCNs are shown in Table I and Figure 1. The PMMA prepared in the absence of clay had a molecular weight of 97,000 g/mol, and the 4% C15a was found to have a molecular weight of 806,000 g/mol, an approximately 830% increase. There appeared to be a trend between the weight percentage of clay and the molecular weight of the matrix PMMA, which can be seen more clearly in the plot of the weight percentage of clay versus the molecular weight (see Fig. 1). The graph shows that as the weight percentage of clay increased so did the molecular weight until a clay loading of 0.5 wt % was reached. Above 0.5 wt %, the molecular weight plateaued around 800,000 g/mol. This plateau was unusual, as one would expect that the clay would continue to alter the molecular weight of the PMMA matrix as the clay loading was increased. This suggests that there was a limiting factor preventing any further increase in the molecular weight.

Solomon and Swift[38] carried out an investigation into the effect of various mineral types (including montmorillonite) in the chain termination of free-radical polymerizations. They found that, in the presence of the mineral, there was an increase in the molecular weight of the polymer and suggested that this was caused by the preferential absorption of the initiating or propagating free radicals onto the Lewis acid sites found on the rim of the clay. Once absorbed by the Lewis acid site, termination was thought to occur via an electron-transfer mechanism. Although montmorillonite was not the most reactive of the minerals studied, it was still found to have a significant effect on the molecular weight.

Such a termination of the radicals of the propagating PMMA chains by the clay could account for an increase in the molecular weight; however, this did not explain why, in our case, the molecular weight plateaued at 0.5 wt % clay. Furthermore, whereas termination by the clay might explain the molecular weight increase seen by Solomon and Swift,[38] it could not account for the large increase associated with the addition of much smaller amounts of clay observed in this study. Solomon and Swift[38] reported a 220% increase in the molecular weight with the addition of 7 wt % unmodified montmorillonite. We observed an 830% increase with the addition of 0.5 wt % modified C15a, which suggested that the change in molecular weight may not have been due to the termination of the PMMA chains. As an alternative explanation, we investigated whether the CTA was reacting preferentially with the clay, resulting in the large increase in the molecular weight, and explaining the plateau effect seen. Polymerizations of 0, 0.25, and 2 wt % clay in the absence of CTA were carried out, and the resulting molecular weights are shown in Table II, along with the data from the analogous reactions carried out with CTA.

A molecular weight of 855,000 g/mol was obtained from the polymerization of MMA in the absence of clay and CTA. This was much higher than the molecular weight observed for PMMA with CTA and showed the large influence that the CTA had on the molecular weight. Furthermore, the molecular weight obtained for PMMA polymerized in the absence of CTA (and clay) was very similar to the

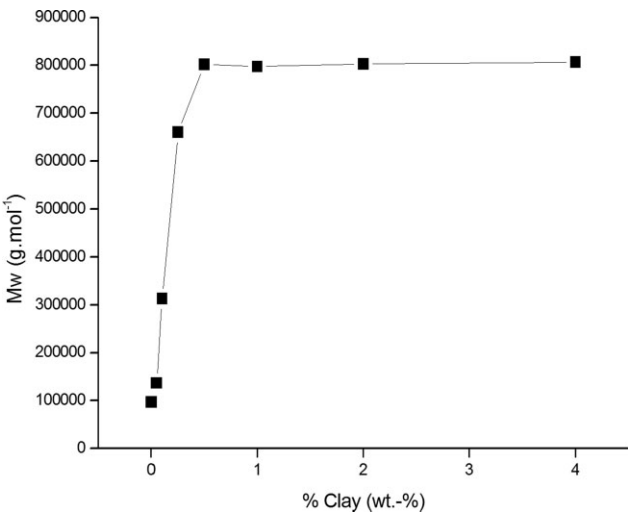

Figure 1 Plot of the weight percentage of clay versus the molecular weight, which shows the plateau effect in the molecular weight.

TABLE II
Effect of CTA on the Molecular Weight of the PMMA and PMMA/C15a Nanocomposites

	Clay (wt %)	CTA (mmol)	M_w (g/mol)	M_n (g/mol)	PDI
PMMA	0	9.9	97,000	54,000	1.8
PMMA (no CTA)	0	0	855,000	243,000	3.5
2% C15a (no CTA)	2	0	807,000	239,000	3.4
2% C15a	2	9.9	803,000	220,000	3.7
0.25% C15a (no CTA)	0.25	0	783,000	329,000	2.4
0.25% C15a	0.25	9.9	660,000	234,000	2.8
0.25% C15a (4g of CTA)	0.25	19.8	458,000	165,000	2.8

M_n = number-average molecular weight.

plateau value of the molecular weight obtained for the PCNs. The 2% C15a (no CTA) sample had a molecular weight of 806,000 g/mol, which was almost identical to that of the 2% C15a (with CTA); this signified that, in this case, that the presence of CTA appeared to have no effect. This suggested that the presence of the CTA was somehow negated by the clay. As postulated previously, we believe that the Lewis acid sites on the clay rim reacted with the thiol radicals from the CTA and terminated the radical. Furthermore, it appeared that, at low loadings of clay (<0.5 wt %), there was insufficient clay present to remove all of the CTA. Figure 1 clearly shows that, as the clay concentration increased, there was a gradual increase in the molecular weight, which suggests a decreasing amount of active CTA. Eventually, a point was reached where there was sufficient clay (0.5 wt %) to react with all of the CTA, and the molecular weight plateaued. A closer look at the molecular weight values showed that there was a slight increase in the molecular weight from 0.5 to 4 wt %. This smaller increase may have been caused by a termination of the propagating PMMA chains by the remaining Lewis acid sites on the clay after the reaction with the CTA. This could also explain why the 2% C15a without CTA had a slightly larger molecular weight than the 2% C15a with CTA.

To further investigate the relationship between the molecular weight, clay loading, and CTA and with a view to lowering the molecular weight of the PMMA in the PCNs, a polymerization with a clay loading of 0.25 wt % was carried out with double the usual amount of CTA. An amount of 0.25 wt % clay was chosen because this amount of clay resulted in a PMMA molecular weight just below the plateau, so the effect of CTA concentration could be most clearly seen. The molecular weights are given in Table II. As expected, there was a linear relationship between the amount of CTA and the molecular weight. The 0.25% C15a without CTA had a molecular weight of approximately 800,000 g/mol, which brought it into line with those with higher clay loadings; with 9.9 mmol CTA, the molecular weight dropped to 660,000 g/mol, and with 19.8 mmol CTA, the molecular weight was further reduced to 460,000 g/mol.

TABLE III
Basal Spacings Calculated from the XRD of PMMA/C15a Nanocomposites Containing Different Weight Percentages of Clay

	Clay (wt %)	d_{001} (nm)
C15a	—	3.2
0.05% C15a	0.05	3.4
0.1% C15a	0.1	3.5
0.25% C15a	0.25	3.6
0.5% C15a	0.5	3.7
1% C15a	1	3.7
2% C15a	2	3.7
4% C15a	4	3.7

Morphology

The basal spacing, or the d_{001} values, for the PCNs were obtained by XRD and are shown in Table III. The XRD traces of PMMA, 0.1% C15a and 4% C15a are shown in Figure 2. An average basal spacing of 3.7 nm was seen and was related to an increase of 0.55 nm compared to C15a clay (3.15 nm); this suggested that the polymer chains entered the clay gallery and swelled the clay. However, the chains were expected to be in an unfavorable conformation because the increase in the basal spacing was less than radius of gyration (R_g). Again by comparing the basal spacing with the clay loading, we saw it initially increased with increasing clay loading but plateaued at 3.7 nm and above 0.5 wt %. The reason for the increase in d_{001} is unknown, but because it

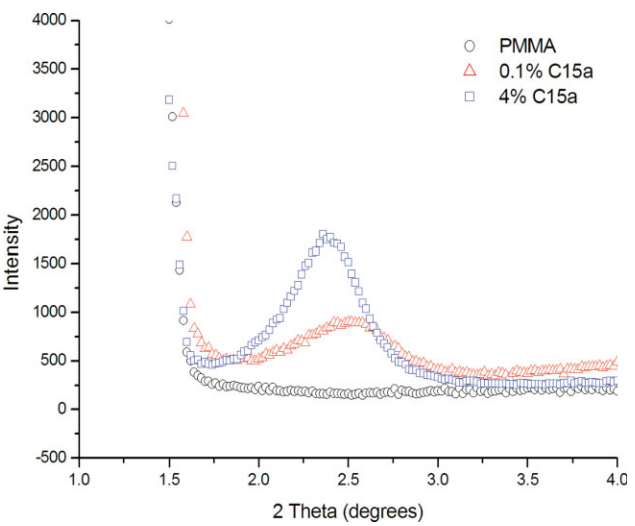

Figure 2 XRD traces of PMMA with 0.1 and 4% C15a. [Color figure can be viewed in the online issue, which is available at www.interscience.wiley.com.]

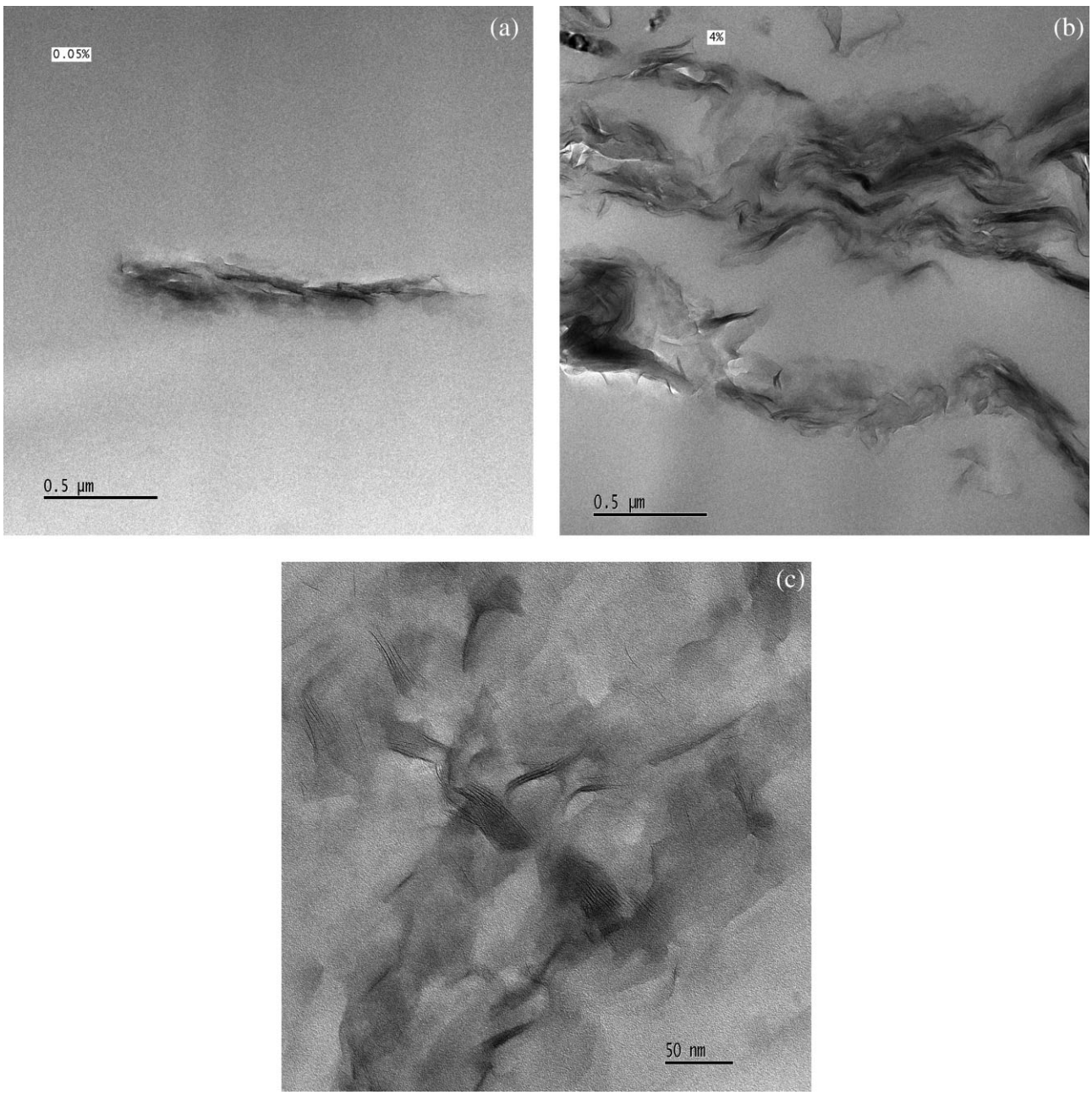

Figure 3 TEM images of (a) 0.05 and (b) 4% C15a on a 0.5-μm scale and of (c) 4% C15a on a 50-nm scale.

followed the same trend as the molecular weight, it may have been due to the increase in the size of the chains found inside the clay gallery.

To gain further understanding of the morphologies, TEM images were taken from small sections of the PCNs. Figure 3(a,b) shows the micrographs of 0.05 and 4% C15a, respectively, and confirm that the nanocomposite had an intercalated morphology. Figure 3(b) shows that the aggregates themselves appeared to be collected together, with areas of unmodified PMMA matrix left, which gave the material a two-phase appearance. Further magnification of 4% C15a [Fig. 3(c)] showed that, in the clay/PMMA phase, the aggregates were in fact well dispersed with aggregate sizes ranging from 3 to 10, and some individual platelets were also clearly visible. The technique used to synthesize the PMMA nanocomposites produced a good dispersion of clay in the PMMA clay phases; however, further mixing was required to achieve good dispersion throughout the whole material to achieve a percolated network.

Rheology

The linear rheology curves are shown in Figure 4; there was little difference between the PCNs

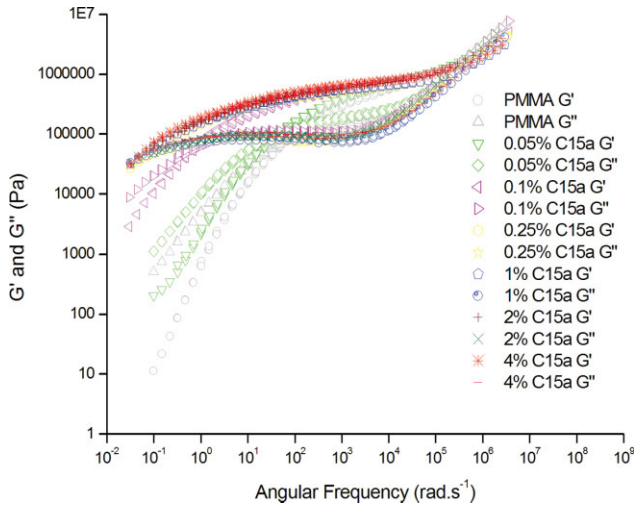

Figure 4 Oscillatory shear rheology plots of the PMMA and PMMA/C15a nanocomposites after time–temperature superposition was applied. A reference temperature of 230°C was used. [Color figure can be viewed in the online issue, which is available at www.interscience.wiley.com.]

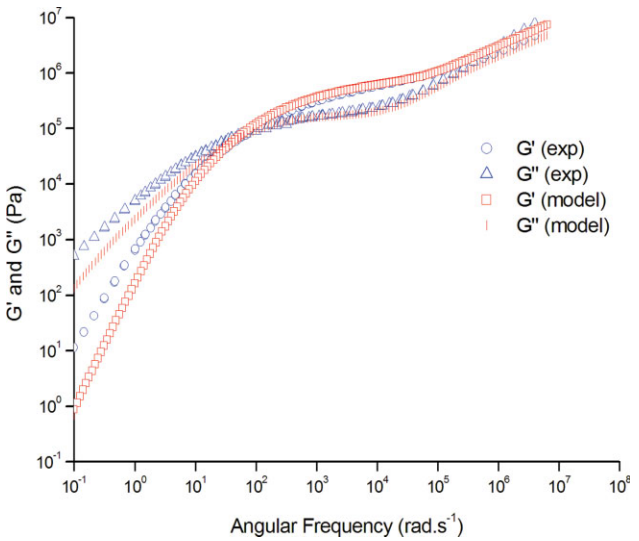

Figure 5 Comparison of the model and experimental rheological data for PMMA. [Color figure can be viewed in the online issue, which is available at www.interscience.wiley.com.]

containing 0.5, 1, 2, and 4 wt % clay; however, 0.1 and 0.05 wt % amounts clearly showed different behavior from those with higher clay loadings, but even for these low clay loadings, there was an increase in G' and G'' compared to unfilled PMMA.

The high frequency range of the rheological data for all of the samples overlapped and the high frequency crossover point is referred to as the entangled τ_R. This crossover and subsequent higher frequency data points were the result of relaxations on a subchain level and were unaffected by the molecular weight. The crossover of G' and G'' in the lower frequency region corresponded to τ_{rep}. Figure 4 shows the increase in τ_{rep} with the addition of clay, which may have been caused by the restriction of reptation due to the clay or by the increase in molecular weight.

The model by des Cloizeaux[30] as used by van Ruymbeke et al.[29] was used to predict the rheology of the PCNs on the basis of their molecular weight distributions. The three relaxation times (τ_{rep}, τ_i, and τ_R) are related to molecular weight by

$$\begin{aligned} \tau_{rep} &= K_{rep}M^3 \\ \tau_i &= K_iM^2 \\ \tau_R &= K_RM^2 \end{aligned} \quad (4)$$

where K_{rep}, K_i, and K_R are all constants and for PMMA at 230°C were found to take on the following values: $K_{rep} = 8.0 \times 10^{-17}$ s/Da^3, $K_i = 6.6 \times 10^{-13}$ s/Da^2, and $K_R = 8.6 \times 10^{-13}$ s/Da^2.

The other parameter required in the model is G_N^0. The literature values for the entanglement molecular weight, which is related to the plateau modulus, range from 5000 to 10,000 g/mol[30,33,39,40] for PMMA. Carrot and Guillet[40] suggested such variation in the entanglement molecular weight and G_N^0 was due to thermal variations and molecular weight differences. Because of these factors, the G_N^0 value used was found from our experimental data for PMMA to have a value of 7.6×10^5 Pa.

The predicted rheological data for PMMA is shown in Figure 5. The model showed good agreement with the experimental data, especially around the plateau region with the reptation crossover points aligning. The model started to fail in the

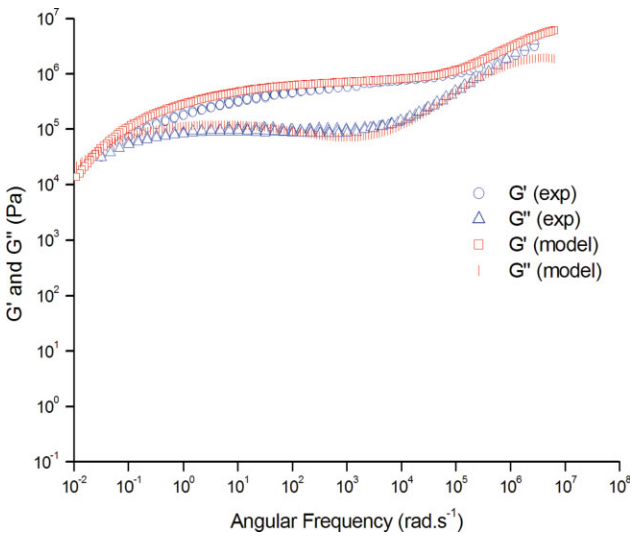

Figure 6 Comparison of the model and experimental rheological data for 4% C15a. [Color figure can be viewed in the online issue, which is available at www.interscience.wiley.com.]

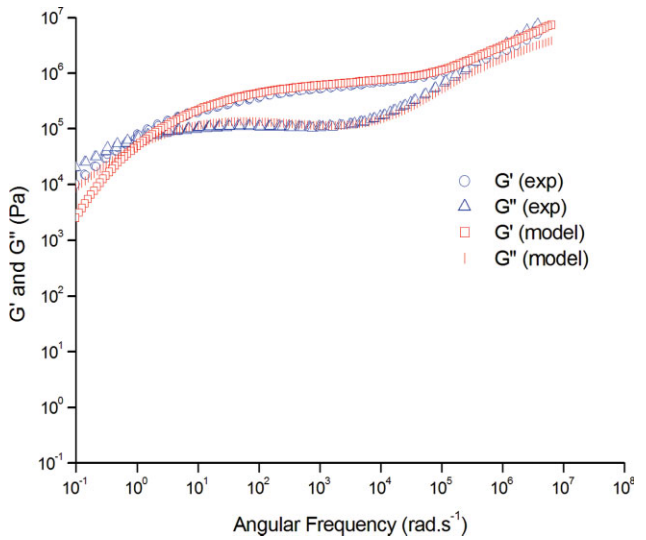

Figure 7 Comparison of the model and experimental rheological data for 0.1% C15a. [Color figure can be viewed in the online issue, which is available at www.interscience.wiley.com.]

lower terminal region, and we believe this was caused by the failure of the Schwarzl relation.[35] The model was also applied to the 4 and 0.1% C15a samples. All of the parameters were kept constant, but the molecular weight data of the respective samples, obtained via SEC, were fed into the model. The comparison between the model and experimental data for 4 and 0.1% C15a are shown in Figures 6 and 7, respectively.

Again, the model showed good agreement with the 0.1 and 4% experimental data. For 4% C15a, the model showed a large plateau region and a long τ_{rep}, which was present in both of the experimental data. The value of the modulus was in good agreement with the experimental one; however, the theoretical modulus started to fall away at the low-frequency end, which was again believed to be cause by the failure of the Schwarzl relation. As there were no significant differences between the experimental and predicted rheological data, we concluded that the changes in the rheological properties with the addition of the C15a clay were justified by the changes in the weight-average molecular weight (M_w) and PDI alone and that the clay did not contribute to the changes in the rheology seen between PMMA and the PMMA/C15a samples.

CONCLUSIONS

We prepared a series of PCNs from PMMA and an organically modified clay, C15a, using an *in situ* suspension polymerization technique. By increasing the amount of C15a present in the suspension polymerization, we observed an increase in the molecular weight of the PMMA matrix, and the molecular weight was found to plateau with a value of approximately 800,000 g/mol with loadings of greater than 0.5 wt % C15a. The polymerization of the matrix PMMA carried out in the absence of CTA produced similar molecular weights, which suggests that the CTA was made inactive during the polymerization and that the cause of the increase in the PMMA molecular weight was reaction of the CTA with the Lewis acid sites situated on the rim of the clay. Above 0.5 wt % clay, there was sufficient clay to react with all of the CTA, which resulted in the plateauing of the molecular weight. On closer inspection of the plateau region (Fig. 1), a slight increase in the molecular weight was seen, which was possibly caused by the termination of the PMMA chains by the clay.

The TEM data showed that a good degree of dispersion was obtained during the suspension polymerization process, although there were still regions where no clay was present, which prevented the formation of percolated networks. The shifting of the reptation time to lower frequencies, as seen by oscillatory shear rheology, might have been an indication of a reinforcing effect caused by the formation of a network of clay platelets. However, modeling the rheological data for the matrix PMMA of the PCNs and including the PDI effects showed good agreement between the predicted rheological and experimental data. This agreement demonstrated that the shift in the reptation time was caused by changes in the molecular weight of the PMMA matrix rather than the partial formation of a percolated network in the PCNs.

This study highlighted the fact that possible side reactions during the polymerization of a matrix polymer caused by the reactivity of the clays should be considered when one contemplates the preparation of PCNs with clays present during the polymerization. This study also demonstrated the need for thorough characterization of such PCNs. Rheology is often used to suggest the positive effects of clays in nanocomposites. Although we anticipated a demonstrable benefit from the inclusion of clay in the PMMA matrix, the careful combination of SEC and theoretical and experimental rheology showed unequivocally that, in this instance, the clays were not responsible for the changes in rheology.

The authors thank R. Lees from Intertek for producing the TEM images and I. Fraser, N. Kirtley, and L. Minto for their advice throughout this project.

References

1. Pavlidou, S.; Papaspyrides, C. D. Prog Polym Sci 2008, 33, 1119.

2. Ray, S. S.; Maiti, P.; Okamoto, M.; Yamada, K.; Ueda, K. Macromolecules 2002, 35, 3104.
3. Chen, B.; Evans, J. R. G.; Greenwell, H. C.; Boulet, P.; Coveney, P. V.; Bowden, A. A.; Whiting, A. Chem Soc Rev 2008, 37, 568.
4. Essawy, H.; Badran, A.; Youssef, A.; Abd El-Hakim, A. E. Polym Bull 2004, 53, 9.
5. Zanetti, M.; Camino, G.; Thomann, R.; Mullhaupt, R. Polymer 2001, 42, 4501.
6. Noh, M. W.; Lee, D. C. Polym Bull 1999, 42, 619.
7. Jang, B. N.; Wilkie, C. A. Polymer 2005, 46, 2933.
8. Zhu, J.; Start, P.; Mauritz, K. A.; Wilkie, C. A. Polym Degrad Stab 2002, 77, 253.
9. Gilman, J. W. Appl Clay Sci 1999, 15, 31.
10. Sahoo, P. K.; Samal, R. Polym Degrad Stab 2007, 92, 1700.
11. Goodarzi, V.; Monemian, S. A.; Angaji, M. T.; Motahari, S. J Appl Polym Sci 2008, 110, 2971.
12. Agag, T.; Koga, T.; Takeichi, T. Polymer 2001, 42, 3399.
13. Rao, Y. Q.; Pochan, J. M. Macromolecules 2007, 40, 290.
14. Tiwari, R. R.; Natarajan, U. Polym Int 2008, 57, 738.
15. Cui, L.; Tarte, N. H.; Woo, S. I. Macromolecules 2008, 41, 4268.
16. Huang, X. Y.; Brittain, W. J. Macromolecules 2001, 34, 3255.
17. Meneghetti, P.; Qutubuddin, S. Thermochim Acta 2006, 442, 74.
18. Li, Y.; Zhao, B.; Xie, S. B.; Zhang, S. M. Polym Int 2003, 52, 892.
19. Potschke, P.; Fornes, T. D.; Paul, D. R. Polymer 2002, 43, 3247.
20. Brown, D. R.; Rhodes, C. N. Catal Lett 1997, 45, 35.
21. Kim, S. S.; Park, T. S.; Shin, B. C.; Kim, Y. B. J Appl Polym Sci 2005, 97, 2340.
22. Lee, D. C.; Jang, L. W. J Appl Polym Sci 1996, 61, 1117.
23. Tabtiang, A.; Lumlong, S.; Venables, R. A. Eur Polym J 2000, 36, 2559.
24. Meneghetti, P.; Qutubuddin, S. Langmuir 2004, 20, 3424.
25. Weimer, M. W.; Chen, H.; Giannelis, E. P.; Sogah, D. Y. J Am Chem Soc 1999, 121, 1615.
26. Degennes, P. G. J Chem Phys 1971, 55, 572.
27. Doi, M.; Edwards, S. F. The Theory of Polymer Dynamics; Clarendon: Oxford, 1986.
28. Likhtman, A. E.; McLeish, T. C. B. Macromolecules 2002, 35, 6332.
29. van Ruymbeke, E.; Keunings, R.; Stephenne, V.; Hagenaars, A.; Bailly, C. Macromolecules 2002, 35, 2689.
30. des Cloizeaux, J. Macromolecules 1992, 25, 835.
31. des Cloizeaux, J. Europhys Lett 1988, 5, 437.
32. Tsenoglou, C. Macromolecules 1991, 24, 1762.
33. Leonardi, F.; Majeste, J. C.; Allal, A.; Marin, G. J Rheol 2000, 44, 675.
34. den Doelder, J. Rheol Acta 2006, 46, 195.
35. Schwarzl, F. R. Rheol Acta 1971, 10, 166.
36. Georgiadou, S.; Brooks, B. W. Chem Eng Sci 2005, 60, 7137.
37. Williams, M. L.; Landel, R. F.; Ferry, J. D. J Am Chem Soc 1955, 77, 3701.
38. Solomon, D. H.; Swift, J. D. J Appl Polym Sci 1967, 11, 2567.
39. Wu, S. J Polym Sci Part B: Polym Phys 1989, 27, 723.
40. Carrot, C.; Guillet, J. J Rheol 1997, 41, 1203.